Building Organometallic Complexes from the Bare Metal: Thermochemistry and Electronic Structure along the Way

P. B. ARMENTROUT

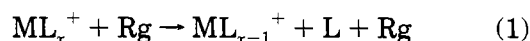*Department of Chemistry, University of Utah, Salt Lake City, Utah 84112*

Introduction

In undergraduate inorganic chemistry, we all learned about the 18-electron rule and ligand field theory (at least for tetrahedral and octahedral fields). These simple, yet powerful ideas enable us to organize a tremendous amount of information regarding *stable* organometallic complexes. Although such stable complexes are the starting materials in organometallic reactions and homogeneous catalysis, the active agents and key intermediates in these systems are coordinately unsaturated transition metal–ligand complexes where one or more ligands have fallen off the stable complex. Clearly, the 18-electron rule no longer applies to such species, and their potential for open-shell character makes their electronic structure less easily organized by the closed-shell rules applicable to 18-electron species. In addition, we rarely know anything about the thermodynamics of such species. In organic chemistry, we learned that we could look up typical C–C, C–H, C–O, etc. bond energies, thus enabling fairly accurate predictions of the thermochemistry of virtually any reaction we desired. We rarely (never?!) encountered such concepts in inorganic chemistry, even though unsaturated complexes cannot be characterized without them.

Why so little progress in characterizing such key species in catalysis? Unsaturated organometallic complexes are reactive (one reason they are good catalysts) and transient, and therefore it is difficult to obtain quantitative information regarding their thermochemistry and electronic structures. For stable precursors, notably carbonyl and alkyl compounds, some thermodynamic information can be obtained from calorimetry (generally by using oxidation or halogenation reactions); however, these data provide only *average* rather than individual bond energies. The latter can vary significantly with the degree of ligation because of changes in the geometric and electronic structures at the metal center. Quantities like the σ-donor and π-acceptor capabilities of various ligands provide only qualitative guides to individual transition metal–ligand bond strengths. The electronic structure of saturated organometallic complexes can be determined ordinarily by spectroscopic means, but these are not routine for transient species such as unsaturated complexes.

In the last several years, a versatile approach has been developed to determine accurate sequential bond dissociation energies (BDEs) for a multitude of metal–ligand systems. This is accomplished by generating individual ML_x^+ (or ML_x^-) complexes in the gas phase and monitoring reaction 1,

$$ML_x^+ + Rg \rightarrow ML_{x-1}^+ + L + Rg \qquad (1)$$

collision-induced dissociation (CID), as a function of the kinetic energy of the reactants in a mass spectrometer. The collision gas, Rg, can be any species but is generally a rare gas atom. Such studies can include virtually any metal (or a cluster of metals)[1] and ligands ranging from familiar species such as CO,[2–8] H_2O,[9–13] NO,[5] alkenes,[14,15] and benzene[16,17] to unusual but potentially important ligands such as N_2,[5,18] CH_4,[12,19] and other alkanes.[20,21]

Although electronic state information is not directly provided by such studies, clues to such information are provided by examination of the sequential BDEs. The basic idea behind this concept is straightforward, although in practice a variety of interactions influence the BDEs. For atomic transition metals, the d orbitals are degenerate and therefore the ground states have high-spin configurations (triplets for d^2 and d^8, quartets for d^3 and d^7, quintets for d^4 and d^6, and sextets

Peter B. Armentrout was born in Dayton, OH, on March 13, 1953. He received his B.S. degree from Case Western Reserve University and a Ph.D. from Caltech, where he worked with J. L. Beauchamp. After a postdoctoral position at Bell Laboratories in Murray Hill, NJ, he joined the faculty at the University of California at Berkeley. In 1987, he moved to the University of Utah, where he is currently professor of chemistry. His other research interests include the application of the techniques described here to simple atom–diatom systems, transition metal clusters, more complicated ligands (such as crown ethers and biologically relevant molecules), and systems of interest in plasma processing of semiconductors.

(1) Ervin, K. M. Work in progress.
(2) Schultz, R. H.; Crellin, K. C.; Armentrout, P. B. *J. Am. Chem. Soc.* **1991**, *113*, 8590.
(3) Khan, F. A.; Clemmer, D. E.; Schultz, R. H.; Armentrout, P. B. *J. Phys. Chem.* **1993**, *97*, 7978.
(4) Sunderlin, L. S.; Wang, D.; Squires, R. R. *J. Am. Chem. Soc.* **1992**, *114*, 2788; **1993**, *115*, 12060.
(5) Khan, F. A.; Steele, D. A.; Armentrout, P. B. *J. Phys. Chem.* **1995**, *99*, 7819.
(6) Meyer, F.; Chen, Y.-M.; Armentrout, P. B. *J. Phys. Chem.* **1995**, *117*, 4071.
(7) Sievers, M.; Armentrout, P. B. *J. Phys. Chem.* **1995**, *99*, 8135.
(8) Goebel, S.; Haynes, C. L.; Khan, F. A.; Armentrout, P. B. *J. Am. Chem. Soc.* **1995**, *117*, 6994.
(9) Magnera, T. F.; David, D. E.; Michl, J. *J. Am. Chem. Soc.* **1989**, *111*, 4100. Magnera, T. F.; David, D. E.; Stulik, D.; Orth, R. G.; Jonkman, H. T.; Michl, J. *J. Am. Chem. Soc.* **1989**, *111*, 5036.
(10) Marinelli, P. J.; Squires, R. R. *J. Am. Chem. Soc.* **1989**, *111*, 4101.
(11) Holland, P. M.; Castleman, A. W. *J. Am. Chem. Soc.* **1980**, *102*, 6174; *J. Chem. Phys.* **1982**, *76*, 4195; Peterson, K. I.; Holland, P. M.; Keesee, R. G.; Lee, N.; Mark, T. D.; Castleman, A. W. *Surf. Sci.* **1981**, *106*, 136.
(12) Schultz, R. H.; Armentrout, P. B. *J. Phys. Chem.* **1993**, *97*, 596.
(13) Dalleska, N. F.; Honma, K.; Sunderlin, L. S.; Armentrout, P. B. *J. Am. Chem. Soc.* **1994**, *116*, 3519.
(14) Schultz, R. H.; Armentrout, P. B. *Organometallics* **1992**, *11*, 828.
(15) Haynes, C. L.; Armentrout, P. B. *Organometallics* **1994**, *13*, 3480.
(16) Chen, Y.-M.; Armentrout, P. B. *Chem. Phys. Lett.* **1993**, *210*, 123.
(17) Meyer, F.; Khan, F. A.; Armentrout, P. B. *J. Phys. Chem.*, accepted for publication.
(18) Tjelta, B. L.; Armentrout, P. B. Work in progress.
(19) Haynes, C. L.; Armentrout, P. B.; Perry, J. K.; Goddard, W. A., III. *J. Phys. Chem.* **1995**, *99*, 6340.
(20) Schultz, R. H.; Armentrout, P. B. *J. Am. Chem. Soc.* **1991**, *113*, 729.
(21) Schultz, R. H.; Armentrout, P. B. *J. Phys. Chem.* **1992**, *96*, 1662.

for d[5]). As ligands are placed around the metal, this degeneracy is broken according to the symmetry of the ligand field. As more ligands are added, the strength of the ligand field increases and the splitting between orbitals increases. Eventually, the difference in orbital energies is larger than the energy required to spin-pair the electrons (an energy that varies from metal to metal) such that the metal—ligand complex adopts a lower spin ground state. When such a spin change occurs, electrons are removed from the higher energy orbitals (those that have the most antibonding character), such that the ligands are bound more tightly. Therefore, spin changes may be observed as anomalous orderings in the sequential BDEs, although a number of factors are also influential in determining these quantities, as discussed below.

Because the gas phase isolates reactive species, unsaturated organometallics can be studied easily. No longer restricted to 18-electron complexes, we can vary the strength of the ligand field systematically by changing the number of ligands, the type of ligands, or both. Also the metal can be varied while the ligand field is held constant, such that periodic trends can be examined easily. Presently, the detailed interpretation of these effects is highly dependent on a synergistic interaction with theoretical results, as will become clear in the following.

Experimental Techniques

The studies described here have been performed on a guided ion beam tandem mass spectrometer described in detail elsewhere.[22] Cationic transition metal complexes are generated in a high-pressure flow tube source.[23] Complexes can be formed either by ionizing stable organometallic precursors or by condensation of the ligand on the bare metal ion, generated by sputtering in a dc discharge of 10% Ar in He. In either method, ions undergo ~10[5] collisions with the room temperature bath gases, which allow three-body stabilization and thermalization of the metal—ligand complexes. The ions are then mass analyzed and focused into a collision cell. Here the ions react with a neutral reagent (at sufficiently low pressures that single ion—neutral encounters are the rule) at a kinetic energy, E, that can be varied over a wide range (3—4 orders of magnitude). Product ions are analyzed in a second mass spectrometer and detected by single particle counting. Ion intensities are converted to absolute reaction cross sections, $\sigma(E)$, a direct measure of the probability of reaction at E. An example of such data is shown in Figure 1 for the case of $Na^+(H_2O)_4$. Cross sections are directly related to rate constants by $k(T) = \langle \sigma v \rangle$ where the brackets indicate integration over a Maxwell—Boltzmann distribution of velocities v. The ability of the ion beam experiment to measure $\sigma(E)$ rather than $k(T)$ is its main distinguishing feature when compared with most other methods for examining ion chemistry.

Temperature of the Ions. Obtaining reliable thermodynamic information from CID experiments depends on knowing *all* the energy available to the reactants. We have demonstrated that internally excited (hot) ions dissociate at lower kinetic energies
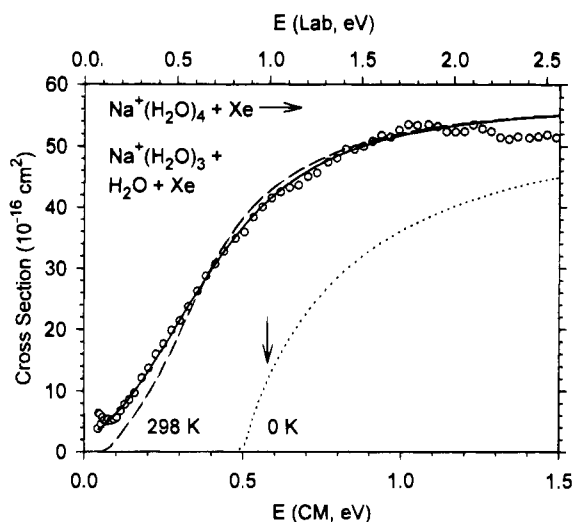
Figure 1. Collision-induced dissociation of $Na^+(H_2O)_4$ as a function of kinetic energy in the center of mass frame (lower x axis) and laboratory frame (upper x axis). Open circles show the cross sections extrapolated to zero collision gas pressure. The best fit of eq 2 is shown as a dashed line for reactants with internal temperatures of 298 K. The solid line shows this model convoluted over the neutral and ionic kinetic energy distributions. The dotted line shows the model cross section for reactants with internal temperatures of 0 K. The intercept of this 0 K model agrees nicely with the threshold (converted to 0 K) determined by equilibrium measurements in ref 40, indicated by the vertical arrow.

than cold ions.[2,24,25] Although it might seem desirable to produce very cold ions using supersonic expansions, there are difficulties in interpreting the resultant data because not all degrees of freedom are cooled equally and the temperature of all modes is difficult to measure. Rather than deal with this uncertainty, we generate ions under thermal equilibrium conditions where the energy in all modes is characterized by a constant temperature, 300 K in our experiments. Although there are no precise methods of directly measuring the ion temperature, the source conditions favor complete thermalization. Results of most of our studies are consistent with this assumption,[2,3,13,26-28] although exceptions associated with failures to completely quench *electronic* excitation have been found.[5,15,29,30] In such cases, more effective cooling reagents can be introduced into the flow gases to remove the excitation.

Analysis of Cross Sections. We analyze the energy dependence of the cross sections for endothermic reactions, such as CID processes, by using the empirical formula 2,[31]

$$\sigma(E) = \sigma_0 \sum g_i (E + E_i - E_0)^n / E \qquad (2)$$

where σ_0 and n are adjustable parameters, E is the relative kinetic energy, and E_0 is the threshold energy. The sum is over all internal states of the reactants

(22) Ervin, K. M.; Armentrout, P. B. *J. Chem. Phys.* **1985**, *83*, 166.
(23) Schultz, R. H.; Armentrout, P. B. *Int. J. Mass Spectrom. Ion Processes* **1991**, *107*, 29.

(24) Hales, D. A.; Armentrout, P. B. *J. Cluster Sci.* **1990**, *1*, 127.
(25) Aristov, N.; Armentrout, P. B. *J. Phys. Chem.* **1986**, *90*, 5135.
(26) Schultz, R. H.; Armentrout, P. B. *J. Chem. Phys.* **1992**, *96*, 1046.
(27) Dalleska, N. F.; Honma, K.; Armentrout, P. B. *J. Am. Chem. Soc.* **1993**, *115*, 12125.
(28) Dalleska, N. F.; Tjelta, B. L.; Armentrout, P. B. *J. Phys. Chem.* **1994**, *98*, 4191.
(29) Fisher, E. R.; Kickel, B. L.; Armentrout, P. B. *J. Chem. Phys.* **1992**, *97*, 4859.
(30) Chen, Y.-M.; Armentrout, P. B. *J. Chem. Phys.* **1995**, *103*, 618.
(31) Armentrout, P. B. In *Advances in Gas Phase Ion Chemistry*; Adams, N. G., Babcock, L. M., Eds.; JAI: Greenwich, 1992; Vol. 1, p 83.

432 *Acc. Chem. Res., Vol. 28, No. 10, 1995*

Armentrout

having energies E_i and populations g_i, where $\Sigma g_i = 1$. Because metal–ligand complexes have many low-frequency vibrational modes (hindered rotations and translations of the stable ligand), the vibrational energy content of the ions is appreciable even at 300 K. It is critical to explicitly include this energy distribution in order to obtain accurate thermochemistry for such species.

The most accurate thermodynamic information is obtained by paying attention to several other details of the analysis. These include the choice of collision gas, Rg in reaction 1 (Xe is used almost exclusively in our studies for reasons described elsewhere),[24,25,32] and the effects of multiple ion–neutral collisions (before analysis, our data are extrapolated to zero neutral pressure, rigorously single collision conditions).[2,33] As the metal–ligand species become larger and more complex, it becomes more likely that they do not dissociate before they are detected (during an experimental time window of $\sim 10^{-4}$ s). If this probability is significant, then the observed onset for dissociation can be delayed, leading to a kinetic shift. We account for this effect by using RRKM theory[34] to calculate a dissociation probability as a function of the ion internal energy.[3,35]

Overall, our analysis of endothermic cross sections starts with eq 2, couples this with the dissociation probability calculated by RRKM theory, and then convolutes the model over the experimental kinetic energy distributions of the cation and neutral reactants.[22] The parameters in eq 2, σ_0, n, and E_0, are varied until the data are accurately reproduced. Detailed examples of this procedure are given elsewhere including an assessment of uncertainties in the E_0 thresholds.[22,31,36] Figure 1 shows an example of the results of this modeling for the case of $Na^+(H_2O)_4$, where the difference between the lines illustrates how large the effect of internal energy can be.

Relationship between CID Thresholds and Bond Energies. If there is no reverse activation barrier, the CID threshold of reaction 1, E_0, equals the bond energy, $D(ML_{x-1}{}^+-L)$. Reverse activation barriers are often absent in ion–molecule processes because of the long-range ion-induced dipole or higher order interactions. Activation barriers can occur when the reaction path is complex,[37] but quantum mechanical considerations show that the potential energy curves are attractive for simple metal–ligand dissociations.[38] Activation barriers have been observed when there are spin or orbital angular momentum restrictions,[31,39] but for transition metal systems, even these restrictions may not apply because of appreciable spin–orbit coupling. Our studies suggest that E_0 does equal the adiabatic BDE, but exceptions have

(32) Loh, S. K.; Hales, D. A.; Lian, L.; Armentrout, P. B. *J. Chem. Phys.* **1989**, *90*, 5466.

(33) Hales, D. A.; Lian, L.; Armentrout, P. B. *Int. J. Mass Spectrom. Ion Processes* **1990**, *102*, 269.

(34) Robinson, P. J.; Holbrook, K. A. *Unimolecular Reactions*; Wiley: London, 1972.

(35) Lian, L.; Su, C.-X.; Armentrout, P. B. *J. Chem. Phys.* **1992**, *97*, 4072.

(36) Armentrout, P. B.; Kickel, B. L. In *Organometallic Ion Chemistry*; Freiser, B. S., Ed.; Kluwer: Dordrecht, 1995; pp 1–45.

(37) Chen, Y.-M.; Clemmer, D. E.; Armentrout, P. B. *J. Am. Chem. Soc.* **1994**, *116*, 7815. Haynes, C. L.; Chen, Y.-M.; Armentrout, P. B. *J. Phys. Chem.* **1995**, *99*, 9110.

(38) Armentrout, P. B.; Simons, J. *J. Am. Chem. Soc.* **1992**, *114*, 8627.

(39) Armentrout, P. B. In *Structure/Reactivity and Thermochemistry of Ions*; Ausloos, P., Lias, S. G., Eds.; Reidel: Dordrecht, 1987; p 97.

Table 1. Sequential Bond Energies of $(H_2O)_{x-1}M^+-H_2O$ (kJ/mol)[a]

M	$x = 1$	$x = 2$	$x = 3$	$x = 4$
Na[b]	95(8)	82(6)	70(6)	55(6)
Mg[b]	119(13)	94(7)	72(9)	48(9)
Al[b]	104(15)	67(5)	64(8)	52(6)
Ti[c]	154(6)	136(5)	67(7)	84(8)
V[c]	147(5)	151(10)	68(5)	68(8)
Cr[c]	129(9)	142(6)	50(5)	51(7)
Mn[c]	119(6)	90(5)	108(6)	50(5)
Fe[c]	128(5)	164(4)	76(4)	50(7)
Co[c]	161(6)	162(7)	65(5)	58(6)
Ni[c]	180(3)	168(8)	68(6)	52(6)
Cu[c]	157(8)	170(7)	57(8)	54(4)

[a] All values are at 0 K with uncertainties in parentheses. [b] Reference 28. [c] Reference 13.
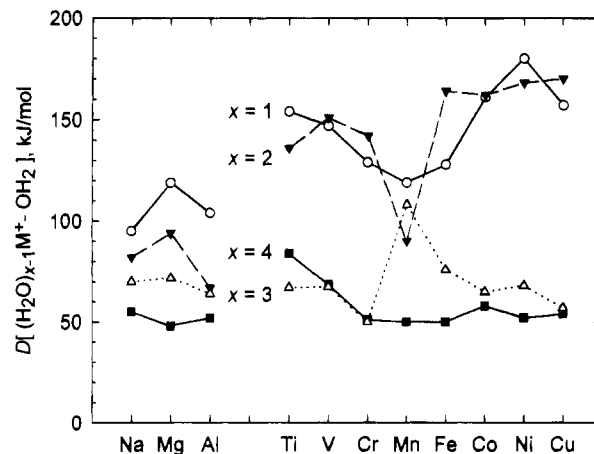

Figure 2. Bond dissociation energies in kJ/mol of metal cation water complexes for one (O), two (▼), three (△) and four (■) water ligands.

been found where dissociation occurs to an excited state asymptote.[2] Because all sources of reactant energy are included in the threshold analysis, the BDEs so determined correspond to thermodynamic values at 0 K.[36]

Main Group Metal–H₂O Ion Complexes

The binding of water molecules to metal ions is the most comprehensively studied gas-phase metal–ligand system. We start by examining the binding of one to four water molecules to simple main group metals: Na^+, Mg^+, and Al^+ ions. Data for the sodium system obtained by CID,[28] Table 1, agree well with those determined by equilibrium methods,[40] and those for the other systems are in good agreement with theory.[41] Such agreement is *not* obtained unless attention is paid to the details of the analysis discussed above. This is illustrated in Figure 1.

Sequential BDEs for $M^+(H_2O)_x$ with M = Na, Mg, and Al decrease as x increases, Figure 2, consistent with metal–ligand bonds that are largely electrostatic. We studied this sequence of metals in order to explore how the BDEs would vary with occupation of the 3s orbital. My naive expectation was that the BDEs would decline because of Pauli repulsion between the 3s electrons and the electrons donated by the water

(40) Dzidic, I.; Kebarle, P. *J. Phys. Chem.* **1970**, *74*, 1466.

(41) Bauschlicher, C. W., Jr.; Langhoff, S. R.; Partridge, H.; Rice, J. D.; Komornicki, A. *J. Chem. Phys.* **1991**, *95*, 5142. Bauschlicher, C. W., Jr.; Partridge, H. *J. Phys. Chem.* **1991**, *95*, 9694. Bauschlicher, C. W., Jr.; Sodupe, M.; Partridge, H. *J. Chem. Phys.* **1992**, *96*, 4453. Sodupe, M.; Bauschlicher, C. W., Jr. *Chem. Phys. Lett.* **1991**, *181*, 321.

ligands. Instead, $Mn^+(3s^1)$ binds H_2O most strongly, followed by $Al^+(3s^2)$, and then $Na^+(3s^0)$. Theory[41] shows that the dipolar water molecule is able to polarize the 3s electron away from the incoming ligand by 3s–3p hybridization. This increases the BDEs because the water ligand interacts with a metal core that has been partially deshielded and hence has moved toward Mg^{2+} and Al^{3+} rather than singly charged cores. The 3s–3p hybridization is less efficient for Al^+ than for Mg^+ because two electrons must be promoted and the energy difference between the 3s and 3p orbitals is larger for Al^+.[28] Theory[41] also notes that this polarization introduces a dipole moment on the metal ion that can favorably interact with the H_2O dipole moment to enhance the bonding.

Geometries of the $M^+(H_2O)_x$ clusters are determined by a principle not unlike the VSEPR (valence shell electron pair repulsion) model of freshman chemistry. For $Na^+(3s^0)$, this means that $Na^+(H_2O)_2$ shows a linear ligand–metal–ligand arrangement; $Na^+(H_2O)_3$ has a trigonal planar metal–ligand geometry; and $Na^+(H_2O)_4$ is tetrahedral. For the $Mg^+(3s^1)$ and $Al^+(3s^2)$ complexes, however, the 3s electron(s) act as another ligand, such that $Mg^+(H_2O)_2$ and $Al^+(H_2O)_2$ have bent ligand–metal–ligand arrangements; $Mg^+(H_2O)_3$ and $Al^+(H_2O)_3$ are nonplanar (near-tetrahedral); and the fourth ligand is believed to begin the second solvent shell.[41] Clearly, the ligand–ligand repulsions are greater for the latter arrangements such that the BDEs for the Mg and Al complexes decrease more rapidly with increasing x than for the Na complexes.

Transition Metal–H₂O Ion Complexes

Both experimental[9–11] and theoretical[42] BDEs for $M^+(H_2O)_x$ (M = Ti–Cu, x = 1 and 2) have been reported, and we have independently checked these results and extended them to include x = 3 and 4,[13] Table 1. Generally good agreement is found among all these studies, although there are a few discrepancies.

Figure 2 shows that the first two water ligands bind to transition metal ions (except for manganese) much more strongly than to sodium, magnesium, and aluminum ions. More intriguing is the observation that the BDEs do not always decrease monotonically with increasing x, in contrast with expectations based on electrostatic interactions.[10] These two observations are largely explained by the ability of the transition metals to use 4s–3dσ hybridization to remove electron density along one axis.[42] This hybridization costs less energy than 3s–3p hybridization but still permits the water ligand to feel a higher nuclear charge. In addition, theory[41] notes that s–dσ hybridization introduces a quadrupole moment on the metal ion that can favorably interact with the H_2O dipole. Unlike 3s–3p hybridization, which moves the electron density to the opposite side of the metal, 4s–3dσ hybridization moves the electron density to an orbital perpendicualr to the metal–ligand axis. Consequently, the second ligand can also see a higher nuclear charge if it approaches from the side opposite the first ligand. Thus, the second bond is also strong and can be

(42) Rosi, M.; Bauschlicher, C. W., Jr. *J. Chem. Phys.* **1989**, *90*, 7264; **1990**, *92*, 1876. Bauschlicher, C. W., Jr.; Langhoff, S. R.; Partridge, H. *J. Chem. Phys.* **1991**, *94*, 2068.
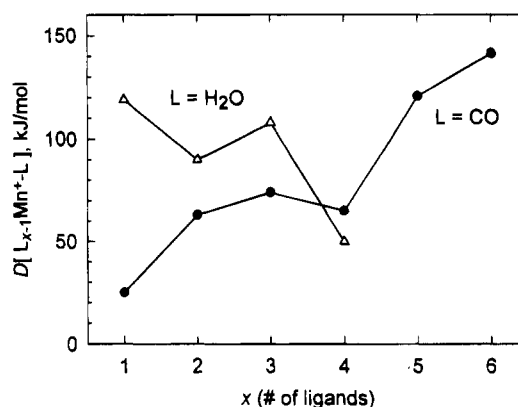

Figure 3. Bond dissociation energies in kJ/mol of manganese cation complexes of water (△) and carbon monoxide (●).

stronger than the first bond, because the first ligand pays the energetic cost of hybridization.

Manganese is an unusual case because its stable $^7S(4s^13d^5)$ ground state does not allow facile hybridization or promotion. Like $Mg^+(H_2O)_2$ and $Al^+(H_2O)_2$, $Mn^+(H_2O)_2$ has a bent ligand–metal–ligand geometry (because the 4s electron is still present and 4s–3dσ hybridization is ineffective because the 4s and 3dσ electrons are high-spin coupled), whereas all other $M^+(H_2O)_2$ complexes of Table 1 have linear geometries (because the metal core is essentially $4s^03d^n$, although both M = Ti and Fe complexes have appreciable $4s^13d^{n-1}$ contributions).[42] For most of these other metals, the atomic ground state configurations are $3d^n$ so that no electronic rearrangement is necessary upon ligand addition. Exceptions are Ti and Fe, but in both cases, the $3d^n$ states are low lying (11 and 22 kJ/mol, respectively)[43] such that the increased binding energy to the $3d^n$ states easily overcomes the energy needed to put the metal into a mixture of this state and the $4s^13d^{n-1}$ ground state. In the case of Fe, one H_2O ligand is insufficient to overcome this promotion energy because the polar H_2O can interact strongly with $Fe^+(^6D,4s^13d^6)$. Two H_2O ligands are sufficient because of the increased steric interactions in the bent ligand–metal–ligand arrangement dictated by the $4s^1$-$3d^6$ metal configuration.

For most transition metals, the third and fourth water BDEs are weaker than the first two and comparable to those for sodium, magnesium, and aluminum, Figure 2. This indicates that the 4s–3dσ hybridization mechanism can no longer be used to remove electron density from positions occupied by ligands.[42] The exception is $Mn^+(H_2O)_3$, which has a larger BDE than $Mn^+(H_2O)_2$ or any other $M^+(H_2O)_3$ species, Figures 2 and 3. This observation can be rationalized if $Mn^+(H_2O)_3$ has a quintet ground state[13] rather than the septet spin calculated for $Mn^+(H_2O)$ and $Mn^+(H_2O)_2$.[42] In essence, this change of spin means that the Mn^+ has a $4s^03d^6$ electron configuration, such that the metal 4s electron–ligand repulsion is removed. The promotion energy to this quintet state is paid by the first two water ligands, as shown by the calculated septet–quintet splitting energy of 18 kJ/mol in $Mn^+(H_2O)_2$,[42] compared to 113 kJ/mol for the atomic ion.[43]

(43) Corliss, C.; Sugar, J. *J. Phys. Chem. Ref. Data* **1982**, *11*, 1.

Table 2. Sequential Bond Energies of $(CO)_{x-1}M^+$–CO (kJ/mol)[a]

M	$x = 1$	$x = 2$	$x = 3$	$x = 4$	$x = 5$	$x = 6$	$x = 7$
Ti*[b]	118(6)	113(4)	100(4)	87(5)	70(4)	74(3)	52(7)
V[c]	113(3)	91(4)	69(4)	86(10)	91(3)	99(7)	50(9)
Cr[d]	90(4)	95(3)	54(6)	51(8)	62(3)	130(8)	
Mn*[e]	25(10)	63(10)	74(10)	65(10)	121(10)	142(10)	
Fe[f]	131(8)	151(14)	66(5)	103(7)	112(4)		
	[153(8)][g]						
Co[h]	174(7)	152(9)	82(12)	75(6)	75(5)		
Ni[i]	178(9)	171(9)	94(4)	73(4)			
Cu[j]	149(7)	172(3)	75(4)	53(3)			
Ag[j]	89(5)	109(4)	55(8)	45(4)			

[a] Values are at 0 K with uncertainties in parentheses. Asterisks (*) indicate preliminary values. [b] Reference 44. [c] Reference 7. [d] Reference 3. [e] Reference 45. [f] Reference 2. [g] The value in brackets is the directly measured value, assumed to correlate with $Fe^+(^4F)$ + CO products. [h] Reference 8. [i] Reference 5. [j] Reference 6.

Transition Metal–Carbonyl Ion Complexes

Experimental BDEs determined in our laboratory by CID measurements for $M^+(CO)_x$ where M = Ti,[44] V,[7] Cr,[3] Mn,[45] Fe,[2] Co,[8] Ni,[5] Cu, and Ag[6] are listed in Table 2. The accuracy of these values is confirmed by favorable comparison with the sum of the BDEs as calculated for the saturated species: $Cr^+(CO)_6$, $Fe^+(CO)_5$, and $Ni^+(CO)_4$. Literature values, obtained from photoionization or electron impact appearance potentials, are generally flawed by kinetic shifts, as discussed in each of our reports. Comparable information for anionic transition metal–carbonyls is also available and has been discussed in detail elsewhere.[4]

The Case of Mn^+. Differences between CO and H_2O as ligands are elucidated clearly by the BDEs to Mn^+, Figure 3. As noted above, the polar H_2O ligand stabilizes the $Mn^+(^7S,4s^13d^5)$ ground state by inducing 4s–4p polarization, leading to a reasonably strong Mn^+–H_2O bond (similar in magnitude and electronic configuration to the Mg^+–H_2O bond). CO is not able to induce such polarization, and 4s–3dσ hybridization cannot occur because the $^5D(4s^03d^6)$ atomic state is too high in energy.[43] Therefore, Pauli repulsion between the ligand and the 4s electron leads to a weak Mn^+–CO BDE (consistent with the naive bonding picture mentioned above). The situation should be worse for the second CO ligand, but we find that the BDE increases. This is rationalized by a change of spin to the quintet,[46] which no longer has the 4s electron. Note that the spin of MnL_x^+ changes from a septet to a quintet when there are two CO ligands, but three H_2O ligands are required.

As more CO ligands are added, the $Mn^+(CO)_x$ BDEs continue to increase, in stark contrast to expectations based on electrostatics. To explain this, we note that $Mn^+(CO)_6$ is an $18e^-$ species with an octahedral geometry and a singlet ground state, $^1A_{1g}$ (t_{2g}^6).[47] Thus, the spin state of the $Mn^+(CO)_x$ complexes must drop to a triplet and then singlet state as ligands are added. This leads to increases in the BDEs as outlined in the Introduction. One guesses that these spin changes probably occur upon addition of the fifth and sixth CO ligands, as the BDEs increase at these points,[48] but this has not been verified at this writing.

(44) Meyer, F.; Armentrout, P. B. Work in progress.
(45) Khan, F. A.; Armentrout, P. B. Work in progress.
(46) Barnes, L. A.; Rosi, M.; Bauschlicher, C. W., Jr. *J. Chem. Phys.* **1990**, *93*, 609.
(47) Beach, N. A.; Gray, H. B. *J. Am. Chem. Soc.* **1968**, *90*, 5713. Burdett, J. K. *J. Chem. Soc., Faraday Trans. 2* **1974**, *70*, 1599.
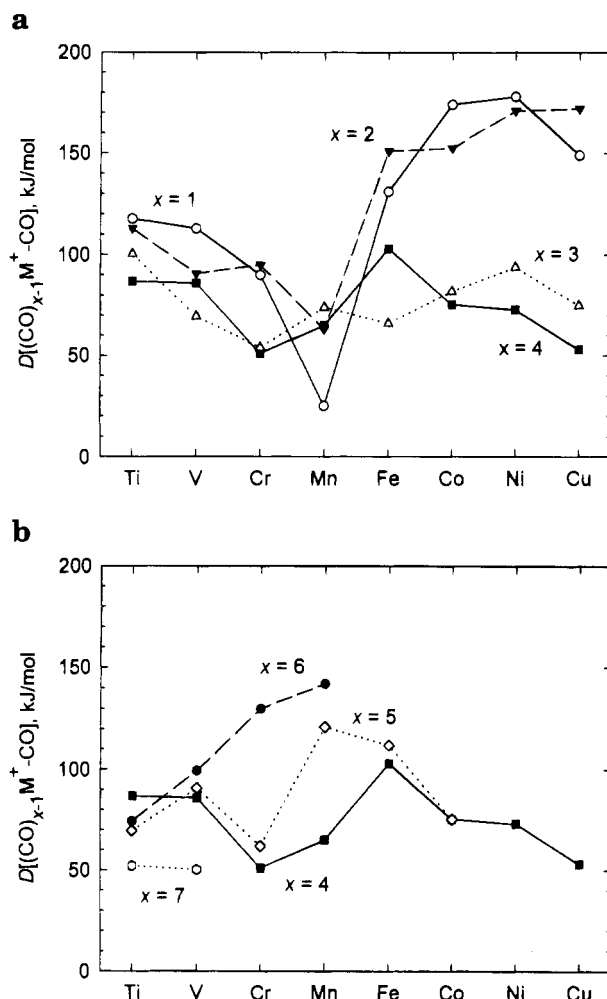
Figure 4. Bond dissociation energies in kJ/mol of first-row transition metal cation carbonyl complexes for one (○), two (▼), three (△), four (■), five (◇), six (●), and seven (○) CO ligands.

$M^+(CO)_x$ ($x = 1$–4) for Other First-Row Transition Metals. Periodic trends in the sequential BDEs of the other $M^+(CO)_x$ complexes are illustrated in Figure 4. There is clearly a tremendous amount of information contained in this plot, and only some of it is easily extracted. Trends in the BDEs for the first several CO ligands are similar in many respects to those already discussed for the $M^+(H_2O)_x$ complexes. One difference is that the first and second BDEs to CO are comparable to those to H_2O for the late transition metals (Fe, Co, Ni, and Cu), while CO binds more weakly to early metals (Ti, V, and Cr). This difference can be rationalized by noting that H_2O is a π-donor that can augment its binding to the early metal ions by interacting with empty 3dπ orbitals. CO is a π-acceptor that favors interacting with the late metal ions where the 3dπ orbitals can be doubly occupied.

$M^+(CO)_x$ ($x = 6$ and 7): Near-Saturated Complexes. For the $M^+(CO)_6$ species, it can be seen that the BDEs gradually increase from M = Ti to Mn. It seems reasonable to conclude that these complexes are all near octahedral (with Jahn–Teller distortions for M = V and Cr), such that the configurations are Ti^+-$(CO)_6$ ($^4A_{1g}$, t_{2g}^3), $V^+(CO)_6$ ($^3T_{1g}$, t_{2g}^4), $Cr^+(CO)_6$ ($^2T_{2g}$, t_{2g}^5), and $Mn^+(CO)_6$ ($^1A_{1g}$, t_{2g}^6). As the t_{2g} orbitals are

(48) In order for this argument to work quantitatively, the low-spin states of the M^+L_{n-1} species must be low lying in energy.

back-bonding with respect to the CO ligand, the increase in BDEs can be directly correlated with a systematic increase in this back-bonding.

We find it straightforward to form the $M^+(CO)_7$ species for M = Ti and V (where the latter is an $18e^-$ species). The BDEs are much stronger than those calculated for ligands in a second ligand shell,[7] but are relatively weak, consistent with extensive steric interactions for a ligand attached to the metal.

$M^+(CO)_x$ (**x = 4 and 5**). If the trend in $M^+(CO)_5$ BDEs is compared with those for $M^+(CO)_6$, Figure 4b, it can be seen that the values are parallel for M = Ti, V, and Mn. Simple molecular orbital calculations[49] can be used to suggest that these pentacoordinate species are square pyramidal (again distortions probably occur for some species, and the trigonal bipyramid structure is fairly close in energy). If so, then the orbital occupations are $Ti^+(CO)_5$ ($^4B_2$, $b_2^1e^2$), $V^+(CO)_5$ ($^3A_1$, $b_2^2e^2$), and $Mn^+(CO)_5$ ($^1A_1$, $b_2^2e^4$). As the b_2 and e orbitals are back-bonding, the increase in BDEs with increasing occupation is easily rationalized again. For $Fe^+(CO)_5$ and $Co^+(CO)_5$, the extra electrons must be added to the antibonding a_1 orbital, thereby explaining why the fifth metal−ligand bond is weakened. Clearly, $Cr^+(CO)_5$ does not fit the pattern analogous to the hexacoordinate complexes. We have suggested that this bond is weak because the dissociation is a spin-forbidden one, that is, a spin change occurs upon addition of the fifth CO ligand to Cr^+ resulting in an anomalous BDE value.[3]

This reasoning can be extended to the tetracoordinate species, where we presume that the molecules are square planar (again simple molecular orbital calculations[49] suggest this for all but the Cu^+ complex where the tetrahedral geometry is clearly preferred). $M^+(CO)_4$ BDEs parallel those for $M^+(CO)_5$ except for M = Mn, Figure 4b. This is consistent with the low-lying metal orbitals being b_{2g} and e_g, which are again back-bonding with respect to the CO ligands. We again speculate that the low BDE for $Mn^+(CO)_4$ can be attributed to a spin change, as noted above.

Weak Field Transition Metal−Ligand Ion Complexes

As noted in the Introduction, gas-phase techniques are not limited to conventional ligands, thereby allowing the examination of very weak field ligands that may be of substantial chemical interest. One example is N_2, isoelectronic with the CO ligand, but incapable of forming the stable $18e^-$ complexes that CO forms, which is of interest in nitrogen fixation. Another is methane, of interest in terms of understanding C−H bond activation.[50,51]

$M^+(N_2)_x$ **Complexes.** We find that four N_2 ligands can be attached to Ni^+ and five to Fe^+.[5,18] BDEs of N_2 to Ni^+, Table 3, follow the same trends as the CO BDEs, but the values are systematically 38 ± 3% lower,[5] consistent with N_2 being a weaker σ-donor and π-acceptor ligand. A similar decrease in BDEs is

(49) Orbital energies are estimated as outlined in refs 3 and 5−8 by using results of Elian and Hoffmann: Elian, M.; Hoffmann, R. *Inorg. Chem.* **1975**, *14*, 1058.

(50) Armentrout, P. B. In *Gas Phase Inorganic Chemistry*; Russell, D. H., Ed.; Plenum: New York, 1989; p 1.

(51) Armentrout, P. B. In *Selective Hydrocarbon Activation: Principles and Progress*; Davies, J. A., Watson, P. L., Liebman, J. F., Greenberg, A., Eds.; VCH: New York, 1990; p 467.

Table 3. Sequential Bond Energies of Weak Field Metal−Ligand Complexes (kJ/mol)[a]

$M^+(L)_x$	x = 1	x = 2	x = 3	x = 4	x = 5
$Fe^+(N_2)_x$[b]	49(10)	93(10)	35(10)	44(10)	71(10)
$Ni^+(N_2)_x$[c]	111(11)	111(11)	56(4)	42(10)	
$Ti^+(CH_4)_x$[d]	70(3)	73(3)	28(6)		
$Fe^+(CH_4)_x$[e]	57(3)	97(4)	99(6)	74(6)	
$Co^+(CH_4)_x$[f]	90(6)	96(5)	40(5)	65(6)	

[a] Values are at 0 K with uncertainties in parentheses. [b] Preliminary values from ref 18. [c] Reference 5. [d] Reference 55. [e] Reference 12. [f] Reference 19.
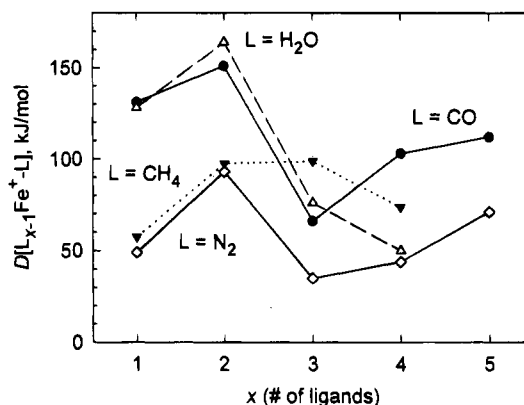

Figure 5. Bond dissociation energies in kJ/mol of iron cation complexes of water (△), carbon monoxide (●), methane (▼), and nitrogen (◇).

found in the preliminary data for $Fe^+(N_2)_x$ complexes, Table 3, but only for x = 2, 3, and 5. $Fe^+(N_2)$ and $Fe^+(N_2)_4$ complexes have BDEs about 60% lower than their CO analogues, Figure 5. Although the details of this observation have not been elucidated as yet, one possibility is that they can be attributed to differences in where the strong-field CO and weak-field N_2 ligands induce spin changes. In the nickel system, no spin changes occur upon ligation and the differences in CO and N_2 BDEs vary systematically. In the iron system, two spin changes are known to occur upon CO ligation,[2] consistent with a variation in two of the relative iron−ligand BDEs.

$M^+(CH_4)_x$ **Complexes.** Table 3 lists the BDEs of one to four molecules of methane bound to Fe^+ and Co^+ as determined by CID studies.[12,19] Our results for Co^+ are in good agreement with theoretical results of Perry et al.[19,52] and equilibrium measurements of Kemper et al.[53] In these complexes, the methane ligands are believed to be intact, as there are no indications that the metal ions have inserted into the CH bonds.

Trends in the $Co^+(CH_4)_x$ BDEs have been explained[19,52] by considering the $4s-3d\sigma$ hybridization effects discussed above. Calculations indicate that if no hybridization were to occur, then the Co^+−methane BDEs would be nearly uniform at ~70 kJ/mol. Hybridization enhances the first two BDEs, and the second is larger than the first because the promotion energy is paid by the first ligand. The third ligand has a very weak BDE because the $4s-3d\sigma$ hybridization enhancement is lost (in essence, this bond energy is 3×70 kJ/mol minus the strong first and second BDEs). The fourth ligand is then bound approxi-

(52) Perry, J. K.; Ohanessian, G.; Goddard, W. A. *J. Phys. Chem.* **1993**, *97*, 5238.

(53) Kemper, P. R.; Bushnell, J.; van Koppen, P.; Bowers, M. T. *J. Phys. Chem.* **1993**, *97*, 1810.

mately by the 70 kJ/mol value associated with no $4s-3d\sigma$ hybridization.

This mechanism for explaining the enhancement of the fourth BDE relative to the third has also been suggested by Ricca and Bauschlicher[54] for $Fe^+(CO)_x$ complexes. While this explanation has merit in both cases, it is unclear whether it is completely valid in either. This is because it should hold for many metal–ligand complexes, but the results shown in Figures 2 and 4 show that the fourth BDE is generally weaker than the third. For Co^+ complexes, only the $L = CH_4$ complexes shows this increase, while $L = CO$ and H_2O do not. For Fe^+ complexes, only the $L = CO$ complexes show this increase, while $L = H_2O$ and CH_4 do not. Indeed, Figure 5 shows that the BDE patterns for Fe^+ complexes of H_2O, CO, N_2, and CH_4 all differ, with the rather unexpected result that $D[(CH_4)_2Fe^+-CH_4]$ exceeds $D[(H_2O)_2Fe^+-H_2O]$ and $D[(CO)_2Fe^+-CO]$.[12] These variations are likely to be a result of electronic reorganization, as discussed above and elsewhere in the literature,[12] and other factors, but the bond energy patterns are not presently understood in detail.

$Ti^+(CH_4)_x$: Cluster-Assisted Reactivity. Very recently, van Koppen et al.[55] measured the binding energy of methane to Ti^+ by using equilibrium methods. Not only do they determine the BDEs listed in Table 3, but they find clear evidence that when a third CH_4 ligand is added to Ti^+, insertion of the metal into a C–H bond competes with simple ligand addition. The rationale for this is clear: the first two ligands provide a sufficiently strong ligand field that the low-spin state of the metal is stabilized. C–H bond activation is then facile as it has been demonstrated that the doublet states of Ti^+ activate methane much more efficiently than the low-lying quartet states.[56]

The implications of such a finding are exciting because this demonstrates that reactivity at metal centers can be influenced (eventually, tuned) by altering the ligand shell surrounding them. Clearly, the ligands need not be the same as the desired reagent (CH_4 in the example above). For example, we have recently determined that H–H, C–H, and C–C bond activation is drastically different for $Fe^+(CO)$ vs Fe^+-(H_2O).[57] Continued studies on the influence of ligation on reactivity are an exciting direction for the future, but an understanding of the results will require the characterization of the unsaturated organometallic complexes used.

Conclusion

It should be clear from this exposition that considerable progress has been made in determining thermochemistry for a variety of unsaturated metal–ligand complexes. Although these methods are restricted to ionic (cation or anion) species, such values can be coupled with measurements of ionization energies (IEs) or electron affinities (EAs) to provide individual BDEs for *neutral* complexes. Indeed, this has been done for a limited number of metal carbonyls by Squires and co-workers.[4] Measurement of the IEs of unsaturated organometallic complexes is certainly technologically possible but is not presently being pursued.

The interpretation of sequential BDEs to determine the electronic characteristics of unsaturated organometallics is in its infancy. Presently, it is difficult to pinpoint where spin changes occur solely on the basis of such thermodynamic information; however, this should be possible in the future on the basis of continued theoretical support on selected systems and experimental spectroscopy in some instances. Intuition gained from these preliminary studies should eventually provide sufficient insight into the most important effects, such that reasonable interpretation of experimental results can be achieved without needing to resort to high-level calculations. The latter seems impractical given the number of molecules and their complexity. Prospects are promising for effectively extending simple ligand-field theory to unsaturated organometallic species, and eventually, for using this knowledge to help "tune" the reactivity of such complexes.

(54) Ricca, A.; Bauschlicher, C. W., Jr. *J. Phys. Chem.* **1994**, *98*, 12899.
(55) van Koppen, P. A. M.; Kemper, P. R.; Bushnell, J. E.; Bowers, M. T. *J. Am. Chem. Soc.* **1995**, *117*, 2098.
(56) Sunderlin, L. S.; Armentrout, P. B. *J. Phys. Chem.* **1988**, *92*, 1209.
(57) Tjelta, B. L.; Armentrout, P. B. *J. Am. Chem. Soc.* **1995**, *117*, 5531; work in progress.